





Accounting for Pipeline Interference and Soil Stratification on Overhead Line Parameters: A Solution for Protective Relays and Fault Locators

Caio M. Moraes ^{*}, *Student Member, IEEE*, Amauri G. Martins-Britto [†], *Member, IEEE*,
Felipe V. Lopes [‡], *Senior Member, IEEE*, Kleber M. Silva [§], *Senior Member, IEEE*

Department of Electrical Engineering, University of Brasília, Brasília, Brazil^{*†§}

Department of Electrical Engineering, Federal University of Paraíba, João Pessoa, Brazil[‡]

Email: caio.missiaggia@aluno.unb.br^{*}

Abstract—This paper presents a methodology for computing the electrical parameters of overhead transmission lines accounting for metallic pipeline interferences and soil stratification effects. The method is based on the closed-form analytical solution of the Carson’s integral, which is used to calculate self and mutual line parameters. The Alternative Transients Program (ATP) is used to simulate a wide variety of short-circuit scenarios on a 230 kV/60 Hz transmission line 200 km long, considering a hypothetical case of interferences with a pipeline and soil stratifications based on resistivity measurements. Obtained results reveal that zero sequence impedance may be significantly affected by uncertainties due to pipeline interferences and soil layered structure, thereby a more robust line parameter calculation in practical applications is required to avoid errors in line protection which uses zero sequence as fundamental parameters.

Keywords—ATP, electromagnetic interferences, line parameters, short circuit, transmission lines.

I. INTRODUCTION

The problem of mutual electromagnetic influences between transmission lines and other metallic structures (such as gas and oil pipelines, fences, railroads etc) still poses challenges to the scientific community. Due to the increasingly restrictive environmental regulations regarding the use of space, cases of interference in right of ways shared by lines and pipelines have become common, which has motivated researches in this area [1], [2], [3].

A metallic pipeline when exposed to the energized conductors of a transmission line is subjected to a variety of phenomena, which results in the rise of metal potential along its path due to inductive, conductive and capacitive coupling mechanisms between

the two structures, in both steady-state (normal operation) and transient (fault cases) regimes [1], [2]. These coupling mechanisms depend on the geometry of the structures, type and arrangement of conductors, voltage and current levels, type of pipeline coating, electrical resistivity of the soil, among other factors. As a consequence, some risks to the integrity of assets (facilities involved) and people arise, such as: electrical shock caused by touch or step voltages, breakdown of the pipeline dielectric coating, metal electrochemical corrosion and damage due to current imposition to the metallic pipe and connected equipment [1].

It should be noted that the presence of a metallic pipeline in the vicinity of a given transmission line also may affect the calculation of its electrical parameters, leading to uncertainties in the model settings taken into account in various monitoring approaches, such as protection and fault location functions.

Another recognized source of error that may affect the calculation of line parameters is the uncertainty of the soil electrical resistivity [4]. Indeed, actual soils are anisotropic media, i.e. their properties vary with direction and depth [5]. Nevertheless, its influence on the classical coupling model is expressed in Carson’s equation by an uniform parameter ρ [6]. Besides, designers usually adopt typical values from soil tables, rather than actually having resistivity surveys and building accurate soil models [7].

An important factor on the aforementioned context regards the methodology used to proceed with the computations of the line parameters. The classical methodology is based on the series expansion of the Carson’s equation, in which the first two terms of the series are usually considered, being the remaining ones

disregarded [6]. This is a convenient and computationally effective approach that produces satisfactory results for low frequencies and for relatively small spacings between mutually coupled conductors, such as the usual distances between phase conductors and neutral wires. However, this simplification tends to introduce significant errors in more complex studies, especially when interferences between transmission lines and underground metallic pipelines are present [1].

From the issues so far, it is concluded that the presence of an interfering metallic structure as well as the improper soil modeling can affect applications that rely on the knowledge of line parameters, such as protective relaying and fault locating procedures. Relevant uncertainties in line parameters may result in mislead settings of protection and fault location devices in situations where the interference and soil stratification is neglected. However, despite the concerns related to such issues, the literature on this problem from the point of view of the impacts on fault location performance is still scarce. Thus, this work presents an improved methodology for calculating transmission line parameters under interference conditions and accounting for the soil layered model. Tests using the software ATP are performed in order to evaluate and demonstrate the impact of these variables on fault location algorithms that depend on the line sequence parameters. The obtained results reveal the performance of some protection and fault location algorithms may be significantly affected if interferences and soil stratification are neglected.

II. MATHEMATICAL MODEL

A. Calculation of Overhead Transmission Line Parameters Under Interference Conditions

For the purposes of this paper, in which the wave propagation phenomenon is not the main concern, the nominal- π model shown in Fig. 1 is sufficiently precise for representing the transmission line. Also, it is worthy to emphasize that the methods proposed in this section remain valid, without loss of generality for the long line model (equivalent- π model), by using the appropriate correction factors in terms of the propagation constant and line length, accordingly to the procedure extensively documented in the literature [8], [9]. Thus, the determination of the series impedances Z and shunt admittances Y for the transmission line model subject to interferences is required.

Figure 2 shows a system comprised of phase conductors, designated by the subscripts a , b and c , neutral wires, identified by the subscripts $n1...nN$ and an underground pipeline, followed by the p subscript. The

series impedance matrix of this system assumes the general form expressed in (1) [9]:

$$\mathbf{Z} = \begin{bmatrix} Z_{a,a} & Z_{a,b} & Z_{a,c} & Z_{a,n1} & \dots & Z_{a,nN} & Z_{a,p} \\ Z_{b,a} & Z_{b,b} & Z_{b,c} & Z_{b,n1} & \dots & Z_{b,nN} & Z_{b,p} \\ Z_{c,a} & Z_{c,b} & Z_{c,c} & Z_{c,n1} & \dots & Z_{c,nN} & Z_{c,p} \\ \vdots & \vdots & \vdots & \vdots & \ddots & \vdots & \vdots \\ Z_{nN,a} & Z_{nN,b} & Z_{nN,c} & Z_{nN,n1} & \dots & Z_{nN,nN} & Z_{nN,p} \\ Z_{p,a} & Z_{p,b} & Z_{p,c} & Z_{p,n1} & \dots & Z_{p,nN} & Z_{p,p} \end{bmatrix} \quad (1)$$

Elements $Z_{i,j}$ outside the main diagonal of the matrix \mathbf{Z} correspond to the mutual impedances between conductors i and j with ground return path, computed in ohms per unit length using Carson's equation (2) [6]:

$$Z_{i,j} = Z_m = \frac{j\omega\mu_0}{2\pi} \ln \left(\frac{D'_{i,j}}{D_{i,j}} \right) + \frac{j\omega\mu_0}{2\pi} \int_0^\infty \frac{2e^{-H\lambda}}{\lambda + \sqrt{\lambda^2 + j\frac{\omega\mu_0}{\rho} - \omega^2\mu_0\epsilon_0\epsilon_r}} \cos(\lambda D) d\lambda, \quad (2)$$

where $\mu_0 = 4\pi \times 10^{-7}$ H/m is the magnetic permeability constant in free space, $\epsilon_0 \approx 8.85 \times 10^{-12}$ F/m is the vacuum electrical permittivity, ρ is the local soil electrical resistivity, in $\Omega \cdot m$, ϵ_r is the local soil relative electrical permittivity, H , D , $D_{i,j}$ and $D'_{i,j}$ are the relative distances represented in Fig. 2, in meters, with: $H = y_i + y_j$, $D = x_j - x_i$, $D_{i,j} = \sqrt{(x_j - x_i)^2 + (y_i - y_j)^2}$ and $D'_{i,j} = \sqrt{(x_j - x_i)^2 + (y_i + y_j)^2}$, being $[x_q, y_q]$, $q = i, j, \dots$ are the coordinates of q -th conductor/pipeline.

Elements $Z_{i,i}$ in the main diagonal are the self impedances of the aboveground conductors, calculated as in (3):

$$Z_{i,i} = Z_s = R_{AC} + \frac{j\omega\mu_0}{2\pi} \ln \left(\frac{2|y_j|}{GMR} \right) + \frac{j\omega\mu_0}{2\pi} \int_0^\infty \frac{2e^{-2|y_j|\lambda}}{\lambda + \sqrt{\lambda^2 + j\frac{\omega\mu_0}{\rho} - \omega^2\mu_0\epsilon_0\epsilon_r}} d\lambda, \quad (3)$$

where R_{AC} is the conductor AC ohmic resistance (supplied by the manufacturer) corrected to the operating temperature, given in ohms per unit length, and GMR is the geometric mean radius of the conductor, as reported by the manufacturer or calculated according to the geometry of the cable bundle, expressed in meters. For the case of a tubular conductor, such as the pipeline depicted in Fig. 3, the geometric mean radius, denoted by GMR_{TU} is determined using (4) [10]:

$$\ln(GMR_{TU}) = \ln(r_{ext}) - \frac{\frac{r_{ext}^4}{4} - r_{ext}^2 r_{int}^2}{(r_{ext}^2 - r_{int}^2)^2} + \frac{r_{int}^4 \left[\frac{3}{4} + \ln\left(\frac{r_{int}}{r_{ext}}\right) \right]}{(r_{ext}^2 - r_{int}^2)^2}, \quad (4)$$

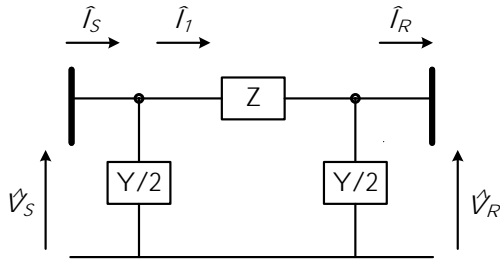
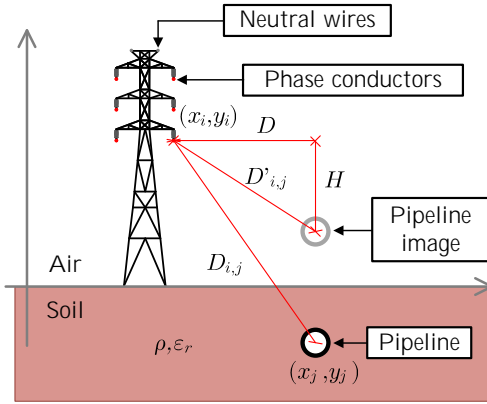

 Figure 1: Nominal- π model of a transmission line.


Figure 2: Phase conductors, neutral wires and pipeline.

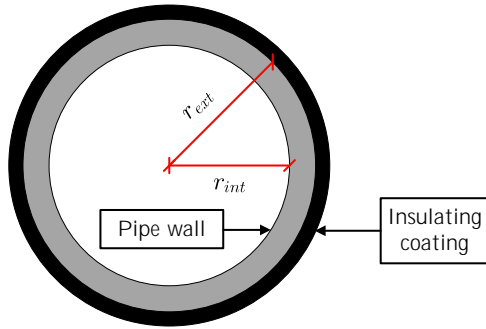


Figure 3: Cross section of a pipeline.

where r_{ext} and r_{int} express, respectively, the external and the internal radius of the tubular pipeline structure, in meters.

The first term in (2) and the second term in (3) correspond to the ground return impedance for a perfectly conductive soil. The improper integrals, known as Carson's integrals, represent the effects of the soil with finite resistivity, including losses caused by current return. The Carson's integral solution has been

assessed by several researchers using numerical techniques based on quadratures, power series expansion or deduction of simplified expressions, being worth mentioning the formulas derived by Carson-Clem, Deri, Lucca and Ametani [1], [11], [12], [13]. The use of simplified formulas is convenient, but may introduce significant errors if the particularities of the interference problem under study are not well understood. In general, these expressions produce satisfactory results for low frequencies and relatively small spacings between conductors, which imposes a limitation to the calculation model.

In [14], Theodoulidis shows that the Carson's integral can be evaluated analytically, with floating-point precision and without convergence problems, by means of a closed-form solution, i.e., expressed in terms of one or more functions whose behavior is well known. Indeed, the integrals in (2) and (3) can be written as (5) with the variable change expressed as shown in (6) and (7):

$$\int_0^\infty \frac{2e^{-H\lambda}}{\lambda + \sqrt{\lambda^2 + j\frac{\omega\mu_0}{\rho} - \omega^2\mu_0\epsilon_0\epsilon_r}} \cos(\lambda D) d\lambda = \frac{\pi}{2u_1} [\widehat{H}_1(u_1) - \widehat{Y}_1(u_1)] - \frac{1}{u_1^2} + \frac{\pi}{2u_2} [\widehat{H}_1(u_2) - \widehat{Y}_1(u_2)] - \frac{1}{u_2^2}, \quad (5)$$

$$u_1 = (H - jD) \sqrt{j\frac{\omega\mu_0}{\rho} - \omega^2\mu_0\epsilon_0\epsilon_r}, \quad (6)$$

$$u_2 = (H + jD) \sqrt{j\frac{\omega\mu_0}{\rho} - \omega^2\mu_0\epsilon_0\epsilon_r}, \quad (7)$$

where \widehat{H}_1 is the Struve function and \widehat{Y}_1 is the Bessel function of the second type, both of first order [14], [?], [?], [?].

Since the interfering pipeline is not energized by the power system, it can be treated in the same way as the neutral conductors in the calculation model. Therefore, nodes related to the neutral conductors and the pipeline can be eliminated from (1) using Kron reduction. For a 3-phase system, considering neutral conductors and the pipeline grounded on both extremities, one can write the following equivalent series impedance matrix:

$$\mathbf{Z}_{EQ} = \mathbf{Z}_{FF} - \mathbf{Z}_{FG} \cdot \mathbf{Z}_{GG}^{-1} \cdot \mathbf{Z}_{GF}, \quad (8)$$

being:

$$\mathbf{Z}_{FF} = \begin{bmatrix} Z_{a,a} & Z_{a,b} & Z_{a,c} \\ Z_{b,a} & Z_{b,b} & Z_{b,c} \\ Z_{c,a} & Z_{c,b} & Z_{c,c} \end{bmatrix}, \quad (9)$$

$$\mathbf{Z}_{FG} = \begin{bmatrix} Z_{a,n1} & \dots & Z_{a,nN} & Z_{a,p} \\ Z_{b,n1} & \dots & Z_{b,nN} & Z_{b,p} \\ Z_{c,n1} & \dots & Z_{c,nN} & Z_{c,p} \end{bmatrix}, \quad (10)$$

$$\mathbf{Z}_{\mathbf{GG}} = \begin{bmatrix} Z_{n1,n1} & \dots & Z_{n1,nN} & Z_{n1,p} \\ \vdots & \ddots & \vdots & \vdots \\ Z_{nN,n1} & \dots & Z_{nN,nN} & Z_{nN,p} \\ Z_{p,n1} & \dots & Z_{p,nN} & Z_{p,p} \end{bmatrix}, \quad (11)$$

$$\mathbf{Z}_{\mathbf{GF}} = \begin{bmatrix} Z_{n1,a} & \dots & Z_{nN,a} & Z_{p,a} \\ Z_{n1,b} & \dots & Z_{nN,b} & Z_{p,b} \\ Z_{n1,c} & \dots & Z_{nN,c} & Z_{p,c} \end{bmatrix}. \quad (12)$$

Assuming the transmission line is transposed, the matrix (8) is rewritten as:

$$\mathbf{Z}_{\mathbf{EQ},\mathbf{T}} = \begin{bmatrix} Z_P & Z_M & Z_M \\ Z_M & Z_P & Z_M \\ Z_P & Z_M & Z_P \end{bmatrix}. \quad (13)$$

where Z_P and Z_M are computed using:

$$Z_P = \frac{\mathbf{Z}_{\mathbf{EQ}}(1,1) + \mathbf{Z}_{\mathbf{EQ}}(2,2) + \mathbf{Z}_{\mathbf{EQ}}(3,3)}{3}, \quad (14)$$

$$Z_M = \frac{\mathbf{Z}_{\mathbf{EQ}}(1,2) + \mathbf{Z}_{\mathbf{EQ}}(2,3) + \mathbf{Z}_{\mathbf{EQ}}(3,1)}{3}. \quad (15)$$

Finally, the sequence impedance matrix \mathbf{Z}_{012} is obtained by applying the Fortescue transformation¹:

$$\mathbf{Z}_{012} = \mathbf{T}^{-1} \cdot \mathbf{Z}_{\mathbf{EQ},\mathbf{T}} \cdot \mathbf{T} \begin{bmatrix} Z_0 & 0 & 0 \\ 0 & Z_1 & 0 \\ 0 & 0 & Z_2 \end{bmatrix}, \quad (16)$$

being

$$\mathbf{T} = \frac{1}{3} \begin{bmatrix} 1 & 1 & 1 \\ 1 & a & a^2 \\ 1 & a^2 & a \end{bmatrix}, \text{ where } a = 1\angle 120^\circ, \quad (17)$$

where Z_0 , Z_1 and Z_2 are, respectively, the zero, positive and negative sequence impedances of the transmission line, in ohms per unit length.

A similar procedure is performed to determine the transmission line admittances. Referring again to the dimensions shown in Figs. 2 and 3, and using the same notation as in the calculations shown so far, the matrix \mathbf{P} is formed with the Maxwell's potential coefficients defined in (19) and (20).

$$\mathbf{P} = \begin{bmatrix} P_{a,a} & P_{a,b} & P_{a,c} & P_{a,n1} & \dots & P_{a,nN} & P_{a,p} \\ P_{b,a} & P_{b,b} & P_{b,c} & P_{b,n1} & \dots & P_{b,nN} & P_{b,p} \\ P_{c,a} & P_{c,b} & P_{c,c} & P_{c,n1} & \dots & P_{c,nN} & P_{c,p} \\ \vdots & \vdots & \vdots & \vdots & \ddots & \vdots & \vdots \\ P_{nN,a} & P_{nN,b} & P_{nN,c} & P_{nN,n1} & \dots & P_{nN,nN} & P_{nN,p} \\ P_{p,a} & P_{p,b} & P_{p,c} & P_{p,n1} & \dots & P_{p,nN} & P_{p,p} \end{bmatrix} \quad (18)$$

$$P_{i,j} = \frac{1}{2\pi\epsilon_0\epsilon_r} \ln \left(\frac{D'_{i,j}}{D_{i,j}} \right). \quad (19)$$

$$P_{i,i} = \frac{1}{2\pi\epsilon_0\epsilon_r} \ln \left(\frac{D'_{i,i}}{r_{ext}} \right). \quad (20)$$

¹Equation (17) shows the Fortescue transformation matrix for an ABC system. For ACB systems, the matrix must be adapted.

By analyzing (19) and (20), which are valid for the 60 Hz frequency, it is observed that the transmission line shunt admittances are determined, essentially, by the configuration of the aboveground conductors and by the electrical permittivity of the medium. Therefore, no influences of interference with underground metallic pipes are expected, since they are immersed in a conductive medium (the ground), which is outside the electrostatic coupling region. Obviously, if interference occurs with metallic pipes above ground level, the transmission line admittances will be affected. Besides, for a low frequency scenario, Maxwell's potential coefficients are unaffected by the soil resistivity. In this section, further calculation steps of shunt admittances are omitted, since they are similar to those shown in (8)-(16).

B. Accounting for the Soil Stratification in the Line Parameters Calculation Model

Fig. 2 depicts a case where the soil is perfectly uniform, with electrical resistivity ρ for all $y \in (0, \infty)$, which is considered in Carson's equations (2)-(3). However, real soils are more complex structures, composed by solid, liquid and gaseous elements, whose electrical resistivity is dependent on the presence of water, particle porosity, type of electrolyte and temperature [5].

In practical situations, the soil electrical resistivity is commonly obtained by the Wenner's method, which consists of taking successive readings of an apparent electrical resistivity value from the surface of the soil in different locations and for several depths [15].

The process of deriving a layered soil model from the apparent resistivity measurements is known as soil stratification. Fig. 4 shows a real soil with several layers with different resistivities ρ_i and thickness h_i , and its corresponding model.

The uniform soil model corresponds to the simple arithmetic mean of the apparent resistivity values. Modeling soils stratified in two or more layers requires more sophisticated numerical methods. The problem of soil stratification is well known in electrical grounding applications [5], as well as the uncertainties inherent to the uniform soil model [16]. The Finite Element method has been increasingly used in solving problems involving multi-layered soils. Although this is a precise approach, it is also computationally expensive. An alternative strategy that has presented valid results in previous studies is to reduce the multi-layered model to a uniform equivalent and apply the classic coupling equations such as the Carson's ones [17].

A multi-layered soil, described by N values of resistivity $[\rho_1, \rho_2, \rho_3, \dots, \rho_N]$ and $N - 1$ thickness values $[h_1, h_2, h_3, \dots, h_{(N-1)}]$, can be reduced to a uniform

$$\sigma_{N-1,N} = \sigma_{N-1} \left[\frac{(\sqrt{\sigma_{N-1}} + \sqrt{\sigma_N}) - (\sqrt{\sigma_{N-1}} - \sqrt{\sigma_N})e^{-2h_{N-1}\sqrt{\pi f \mu_{N-1} \sigma_{N-1}}}}{(\sqrt{\sigma_{N-1}} + \sqrt{\sigma_N}) + (\sqrt{\sigma_{N-1}} - \sqrt{\sigma_N})e^{-2h_{N-1}\sqrt{\pi f \mu_{N-1} \sigma_{N-1}}}} \right]^2, \quad (21)$$

$$\vdots$$

$$\sigma_{m-1,m} = \sigma_{m-1} \left[\frac{(\sqrt{\sigma_{m-1}} + \sqrt{\sigma_{m-1,m}}) - (\sqrt{\sigma_{m-1}} - \sqrt{\sigma_{m-1,m}})e^{-2h_{m-1}\sqrt{\pi f \mu_{m-1} \sigma_{m-1}}}}{(\sqrt{\sigma_{m-1}} + \sqrt{\sigma_{m-1,m}}) + (\sqrt{\sigma_{m-1}} - \sqrt{\sigma_{m-1,m}})e^{-2h_{m-1}\sqrt{\pi f \mu_{m-1} \sigma_{m-1}}}} \right]^2, \quad (22)$$

$$\sigma_{eq} = \sigma_1 \left[\frac{(\sqrt{\sigma_1} + \sqrt{\sigma_{m-1,m}}) - (\sqrt{\sigma_1} - \sqrt{\sigma_{m-1,m}})e^{-2h_1\sqrt{\pi f \mu_1 \sigma_1}}}{(\sqrt{\sigma_1} + \sqrt{\sigma_{m-1,m}}) + (\sqrt{\sigma_1} - \sqrt{\sigma_{m-1,m}})e^{-2h_1\sqrt{\pi f \mu_1 \sigma_1}}} \right]^2, \quad (1 \leq m \leq N-2). \quad (23)$$

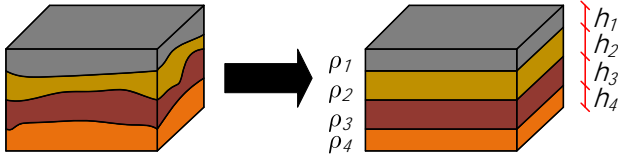


Figure 4: Real soil and stratified model.

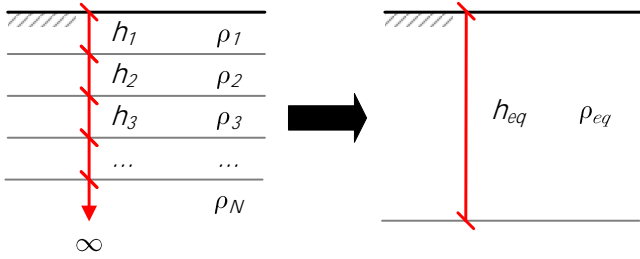


Figure 5: Stratified soil and its equivalent uniform model.

equivalent as described in [18], whose effect is illustrated in Fig. 5.

Considering $\sigma_N = 1/\rho_N$ and f being the power system frequency, in hertz, the presence of multiple layers with different constitutive properties is accounted by replacing the uniform variable σ in Carson equation by the equivalent parameter σ_{eq} , defined as in (21)-(23).

This approach has been proved to provide accurate results yielding a single real-valued parameter that can be readily used with the classic Carson equation (2), therefore being fully compatible with the native ATP routines that handle transmission line parameters [18].

III. CASE STUDY

A transmission system is proposed in Fig. 6, composed of a transmission line connecting two equivalent Thévenin circuits. The model was built in the ATP software to perform short-circuit simulations and obtain the current and voltage waveforms, necessary

for application of the fault location algorithms. The transmission line operates at 230 kV, with a single circuit, horizontal configuration and, under nominal load conditions, with a current of 500 A per phase. It is assumed a perfect transposition of the conductors. The transmission line is 200 km long and shares the right of way with a 8" diameter underground carbon steel pipeline installed at 1.5 m depth, which runs parallel to the transmission line axis along the entire course. Figure 7 shows the geometry of the typical tower the transmission line, indicating the distance from the parallel pipeline, with dimensions in meters.

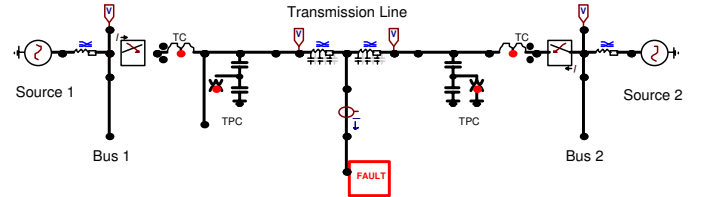


Figure 6: ATP model for the short-circuit simulations.

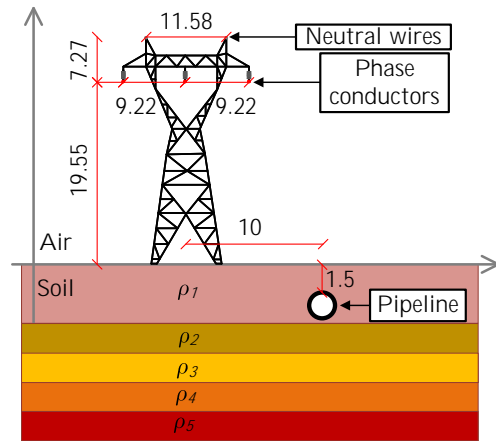


Figure 7: Geometry of the typical tower.

The specifications of the transmission line conduc-

tors are given in Table I. The pipeline characteristics are provided in Table II.

Table I: Specifications of transmission line conductors

Conductor	Description	Temperature
Phases	ACSR 636 MCM 27/7 (Peacock)	50 °C
Neutral	Steel 3/8" HS	50 °C

Table II: Pipeline characteristics

Parameter	Value
Internal radius [m]	0.1014
External radius [m]	0.1095
Electrical resistivity [$\Omega \cdot m$]	1.72×10^{-7}
Magnetic permeability [H/m]	3.77×10^{-4}

In order to exemplify the effect of the soil resistivity, it is used the apparent resistivity data available in Annex B.3 of the standard ABNT NBR 7117, reproduced in Table III, which represent a soil model stratified in five layers, whose parameters are contained in Table IV [15].

Table III: Apparent resistivity measurements as in [15]

Spacing [m]	Apparent resistivity [$\Omega \cdot m$]
1	11938
2	15707
4	17341
8	11058
16	5026
32	3820

Table IV: Five-layered soil model as in [15]

Layer	Resistivity [$\Omega \cdot m$]	Thickness [m]
1	8600	0.64
2	21575	0.29
3	19146	3.47
4	4460	7.4
5	3151	∞

Table V: Resistivity values from uniform models

Model	Resistivity [$\Omega \cdot m$]
IEEE Std. 80 uniform	10815
RESAP uniform	9401.48
Equivalent uniform	3160.89

Table V contains a comparison between three different uniform soil models: 1) the equivalent uniform model, determined using (21)-(23) and the data presented in Table IV; 2) the conventional uniform model,

established under IEEE Std. 80 as the simple arithmetic mean of the apparent resistivity values [16]; and 3) the uniform model obtained using the RESAP module from software CDEGS, which is based on the curve-fitting technique reported in [19].

Applying (21)-(23) to the parameters of the stratified soil given in Table IV, a uniform equivalent soil model with resistivity 3160.89 $\Omega \cdot m$ is obtained, about 29% of the result for a uniform model obtained directly from the apparent resistivity measurements, indicated in Table III. It should also be noted that the uniform equivalent resistivity is very close to the value indicated in Table IV for the deep soil resistivity, which confirms, numerically, reports in the literature that the deep soil resistivity is predominant in studies involving ground return path, and for calculations of mutual couplings in large systems, such as transmission line parameters, the use of the average values of the deep layers often yields satisfactory results for practical purposes [20].

With purpose of to compare the three types of soil models and the influence of interference to calculate TL parameters, six scenarios are studied:

- **Case 1:** considering IEEE Std. 80 uniform soil and no interferences;
- **Case 2:** considering RESAP uniform soil and no interferences;
- **Case 3:** considering uniform soil and no interferences;
- **Case 4:** considering IEEE Std. 80 uniform soil and interference caused by a 10 m parallel pipeline;
- **Case 5:** considering RESAP uniform soil and interference caused by a 10 m parallel pipeline;
- **Case 6:** considering uniform soil and interference caused by a 10 m parallel pipeline;

Finally, Table VI shows the comparison between the scenarios of line parameters calculation, comparing the stratified soil model and considering the presence or not of the pipeline.

Table VI: Line parameters of the case study for each scenario

Cases	Z_1 [Ω/m]	Z_0 [Ω/m]
1	$0.1107 + j0.5337$	$0.5834 + j1.8263$
2	$0.1107 + j0.5337$	$0.5775 + j1.8146$
3	$0.1107 + j0.5337$	$0.5335 + j1.722$
4	$0.1108 + j0.5336$	$0.3819 + j1.3669$
5	$0.1108 + j0.5336$	$0.38 + j1.3628$
6	$0.1108 + j0.5336$	$0.3648 + j1.329$

The case 6 is considered the most relevant scenario and its used as reference for this study. Table VII presents the line parameters errors considering the case 6 as reference.

Table VII: Line parameters errors

Cases	Z_1 Error [%]	Z_0 Error [%]
1	0.142	39.115
2	0.142	38.176
3	0.142	30.809
4	0	2.982
5	0	2.658

Shunt admittances result in the same values for both calculation methods, with $Y_1=3.1034j \mu\text{S/km}$ and $Y_0=2.2324j \mu\text{S/km}$. This is explained by the fact that the capacitance is independent of the soil resistivity and that the interfering pipeline is buried beneath the ground, that is, immersed in a conductive medium and, consequently, absent of electrostatic couplings with the energized conductors of the transmission line. It is relevant to note that the positive sequence parameters do not present considerable differences, with an error of less than 1%. However, the zero sequence impedance is shown to be significantly influenced by interference conditions, in which a discrepancy of 30.81% is observed between the same soil models but with different interference conditions.

The soil model influences in the line parameter, though just presents less than 3% of deviation in zero sequence between the analyzed models and for positive sequence do not present changes.

Tables VIII and IX show the short-circuit currents in the fault branch and its errors for phase-to-ground (AT) simulations occurring at 20%, 40%, 60% and 80% of the transmission line length, that is, 40 km, 80 km, 120 km and 160 km, using the impedance values contained in Table VI for each scenario. The same analyze is performed to phase-to-phase (AB) and the respective results are shown in Table X and XI.

Table VIII: Short-circuit currents for phase-to-ground faults

Cases	m=20%	m=40%	m=60%	m=80%
1	4190.9 A	3180.1 A	3169.5 A	4149.1 A
2	4204.4 A	3191.7 A	3181.1 A	4162.5 A
3	4493.8 A	3371.7	3360.5 A	4449 A
4	4781.7 A	3698.4 A	3686.1 A	4737 A
5	4787.8 A	3703.8 A	3691.5 A	4740 A
6	5061.1 A	3859.2 A	3846.3 A	5010.7 A

Results show that discrepancies between the values of short-circuit currents occur only for the phase-to-ground fault, which is expected, since only the zero sequence parameters present differences when considering the interference conditions and the stratified soil. Thus, problems with monitoring devices are expected

Table IX: Short-circuit errors for phase-to-ground faults

Cases	m=20%	m=40%	m=60%	m=80%
1	17.19 %	17.59 %	17.59 %	17.19 %
2	16.93 %	17.29 %	17.29 %	16.93 %
3	11.21 %	12.63 %	12.63 %	11.21 %
4	5.52 %	4.17 %	4.16 %	5.46 %
5	5.40 %	4.03 %	4.02 %	5.40 %

Table X: Short-circuit currents for phase-to-phase faults

Cases	m=20%	m=40%	m=60%	m=80%
1	6539.8 A	5015.4 A	4998.7 A	6474.6 A
2	6539.6 A	5015.4 A	4998.7 A	6474.6 A
3	6540 A	5015.5 A	4998.8 A	6474.9 A
4	6540.5 A	5016 A	4999.3 A	6475.2 A
5	6540.5 A	5016 A	4999.3 A	6474.9 A
6	6540.7 A	5016.1 A	4999.4 A	6475.5 A

Table XI: Short-circuit errors for phase-to-phase faults

Cases	m=20%	m=40%	m=60%	m=80%
1	0.014 %	0.014 %	0.014 %	0.014 %
2	0.017 %	0.014 %	0.014 %	0.014 %
3	0.011 %	0.012 %	0.012 %	0.009 %
4	0.003 %	0.002 %	0.002 %	0.005 %
5	0.003 %	0.002 %	0.002 %	0.009 %

to arise only in situations in which the fault involves the earth. It should be noted that even for two-phase-to-ground faults, which also involve the earth, monitoring devices do not use zero sequence data, so it can be stated that the impact of pipeline interferences and stratified soil will only exist in events of single-phase short circuits, which, by the way, are the most common in transmission networks.

IV. CONCLUSIONS

Results discussed indicate that the zero sequence line parameters are sensitive to the soil model and the presence of interferences, presenting an error 30.809% smaller in relation to the calculation procedure in which these variables are ignored. The positive sequence parameters are little affected by the soil resistivity and the inductive coupling with other installations.

The discrepancy in the zero sequence impedance propagates to the phase-to-ground short-circuit responses, with an increase of approximately 17.59% in the maximum current in the fault branch for the evaluated cases. This value corresponds to about 600 A, an error that is considerably higher than the permissible tolerances for protection devices. There are

no significant changes in the cases of phase-to-phase short-circuits.

From the above, it is considered of fundamental importance that, in transmission line design, short-circuit studies, dimensioning and calibration of protection and fault location devices, precise numerical methods are used to calculate the electrical parameters. However, it is also necessary to ensure the quality of the field gathered information, especially soil resistivity measurements and the survey of interferences with other facilities.

References

- [1] WG-36.02, "Publication n. 95 - Guide on the Influence of High Voltage AC Power Systems on Metallic Pipelines," Paris, pp. 1-135, 1995. [Online]. Available: <http://www.e-cigre.org/Order/select.asp?ID=96>
- [2] G. C. Christoforidis, D. P. Labridis, and P. S. Dokopoulos, "A hybrid method for calculating the inductive interference caused by faulted power lines to nearby buried pipelines," *IEEE Transactions on Power Delivery*, vol. 20, no. 2, pp. 1465-1473, April 2005.
- [3] L. Qi, H. Yuan, L. Li, and X. Cui, "Calculation of interference voltage on the nearby underground metal pipeline due to the grounding fault on overhead transmission lines," *IEEE Transactions on Electromagnetic Compatibility*, vol. 55, no. 5, pp. 965-974, Oct 2013.
- [4] S. Das, S. Santoso, A. Gaikwad, and M. Patel, "Impedance-based Fault Location in Transmission Networks: Theory and Application," *IEEE Access*, vol. 2, pp. 537-557, 2014.
- [5] J. He, R. Zeng, and B. Zhang, *Methodology and Technology for Power System Grounding*, 2012.
- [6] J. R. Carson, "Wave Propagation in Overhead Wires with Ground Return," *Bell Syst. Tech. J.*, vol. 5, pp. 539-554, 1926.
- [7] E. Whelan, J.M.; Hanratty, B.; Morgan, "Earth Resistivity in Ireland," in *CDEGS Users' Group*, Montreal, 2010, pp. 155-164.
- [8] H. Saadat, *Power System Analysis*, 2nd ed., McGraw-Hill, Ed., 1999.
- [9] J. J. Grainer and W. Stevenson, *Power System Analysis*, 1994. [Online]. Available: <http://medcontent.metapress.com/index/A65RM03P4874243N.pdf>
- [10] H. L. Seneff, "Study of the Method of Geometric Mean Distances Used in Inductance Calculations," 1947.
- [11] G. Deri, A., Tevan, "The Complex Ground Return Plane - A Simplified Model for Homogeneous and Multi-Layer Earth Return," no. August, pp. 31-32, 1981.
- [12] G. Lucca, "Mutual Impedance between an Overhead and a Buried Line with Earth Return," in *Proc. Int. Electr. Eng. 9th Int. Conf. EMC*, no. 1, 1994, pp. 80-86.
- [13] A. Ametani, T. Yoneda, Y. Baba, and N. Nagaoka, "An Investigation of Earth-Return Impedance Between Overhead and Underground Conductors and Its Approximation," *IEEE Transactions on Electromagnetic Compatibility*, vol. 51, no. 3, pp. 860-867, 2009. [Online]. Available: <http://ieeexplore.ieee.org/lpdocs/epic03/wrapper.htm?arnumber=4914803>
- [14] T. Theodoulidis, "On the Closed-Form Expression of Carson's Integral," *Periodica Polytechnica, Electrical Engineering*, vol. 59, no. 1, pp. 26-29, 2015.
- [15] ABNT, "NBR 7117 - Medição da Resistividade e Determinação da Estratificação do Solo," pp. 1-72, 2012.
- [16] IEEE Std 80, "Guide for Safety In AC Substation Grounding," pp. 1-192, 2000.
- [17] A. G. L. Furlan, "Estudo de Interferências Eletromagnéticas entre Linhas de Transmissão e Dutos Enterrados," Dissertação (Mestrado), Universidade Federal de Santa Catarina, 2015.
- [18] A. G. Martins-Britto, F. V. Lopes, and S. R. M. J. Rondineau, "Multi-layer Earth Structure Approximation by a Homogeneous Conductivity Soil for Ground Return Impedance Calculations," *IEEE Transactions on Power Delivery*, vol. 8977, no. c, pp. 1-1, 2019.
- [19] F. Dawalibi and C. Blattner, "Earth Resistivity Measurement Interpretation Techniques," *IEEE Transactions on Power Apparatus and Systems*, vol. PAS-103, no. 2, pp. 374-382, 1984. [Online]. Available: <http://ieeexplore.ieee.org/lpdocs/epic03/wrapper.htm?arnumber=4112522>
- [20] R. Southey and F. Dawalibi, "Improving the Reliability of Power Systems with More Accurate Grounding System Resistance Estimates," *Proceedings. International Conference on Power System Technology*, vol. 4, pp. 98-105, 2005. [Online]. Available: <http://ieeexplore.ieee.org/lpdocs/epic03/wrapper.htm?arnumber=1053512>